



Studies on Peri-root Tissue Formation Around New Type Artificial Root Made of Dense Hydroxyapatite

Katsunari Nishihara

Department of Oral Surgery, Faculty of Medicine, University of Tokyo, 7-3-1 Hongo, Bunkyo-ku, Tokyo 113, Japan

(Received 19 February 1992; accepted 15 May 1992)

Abstract: The aim of this study was to examine the wound healing process and tissue development around a new type of artificial root made of dense hydroxyapatite. The newly tailored artificial roots, which have characteristic corrugated configurations with smooth root surfaces, were implanted immediately after extraction of the premolars of adult dogs. After preliminary experiments, the following studies were carried out: for the observation of tissue formation around the artificial root, artificial root with surrounding tissue were extirpated after fixed periods (6–32 weeks) of implantation; to study tissue formation at the artificial root surface, undecalcified specimens with polished surfaces for microanalysis and decalcified specimens for light microscopic observation were prepared after 72 weeks of implantation. The following results were obtained: around the artificial roots in the jawbone, fibrous tissue formation with angled orientation, bone formation resembling alveolar bone proper, and calcified substance formation attaching to the root surface were observed.

INTRODUCTION

Various kinds of dental implants made of newly developed materials, i.e. titanium, alumina, 'Bio-glass', and hydroxyapatite, which have excellent biocompatibility, have been used clinically.^{1–6}

At present, optimal healing around dental implants is considered to be direct, intimate contact with bone tissue, called osseointegration.³ On the other hand, for ideal substitution of a tooth, development of a dental implant (artificial root) with functional peri-implantium has been tried.¹ Recently, some researchers have finally begun to invent artificial roots with functional, supportive, collagenous peri-implantium.^{7,8} It has been reported that even bioinert single crystal alumina has excellent bioadhesiveness with bone marrow and epithelial cells.¹ Therefore, it is thought that by the use of bioactive ceramic, artificial roots having peri-implantium with functional collagenous fibres can be developed.⁸

A new type of artificial root made of hydroxyapatite has been devised which has quite a different joint system to the jawbone from the conventional

dental implant. The artificial roots were clinically applied and good results were obtained during a 5-year follow-up.⁹ By preliminary experiments, root-supporting tissues resembling those of the natural tooth were observed.

In this paper, the author describes investigation of the jointing modality of hydroxyapatite roots to the jawbone through observation by light microscopy and microanalyser. To observe tissue development around the artificial root in jawbone, a short-term experiment was carried out. For the study of calcified material attachment to the artificial root surface, a long-term experiment with adult dogs was also carried out. It was assumed that mesenchymal cells around the artificial root could develop various kind of cells with facility to induce fibrous tissue, bone tissue and calcified substance resembling the cementum.

MATERIALS AND METHODS

New types of artificial roots (4 mm in diameter) made of sintered dense hydroxyapatite, with



Fig. 1. Bone formation around artificial root 1 month after implantation (undecalcified specimens, toluidine blue staining). Fracture of the artificial root is an artifact during the preparation of specimen. ABP — alveolar bone proper; AR — artificial root; FT — fibrous tissue; BV — blood vessel; PL — periodontal ligament.

smooth root surfaces and characteristic conical and corrugated configurations, were fabricated by Asahi Optical Co. Ltd, Tokyo, Japan. The properties of sintered hydroxyapatite ceramics are as follows:

Molecular formula: $\text{Ca}_{10}(\text{PO}_4)_6(\text{OH})_2$
 Melting point: 1650 °C
 Sintered temperature: 1050 °C
 Theoretical density: 3.16 g/cm³
 Relative density: 99.2%
 Bend strength: 220 MPa
 Compressive strength: 500 MPa
 Vickers hardness: 6.0 GPa

Eight adult male dogs were used in this experiment. Artificial roots were implanted at the time of extraction of the lower premolars in the dogs. The roots of the premolars were far shorter and thinner than the artificial roots to be used; therefore, the post-extraction fossa was enlarged using a 4-mm-diameter burr, corresponding to the artificial root shape. To observe newly developing peri-artificial root tissue

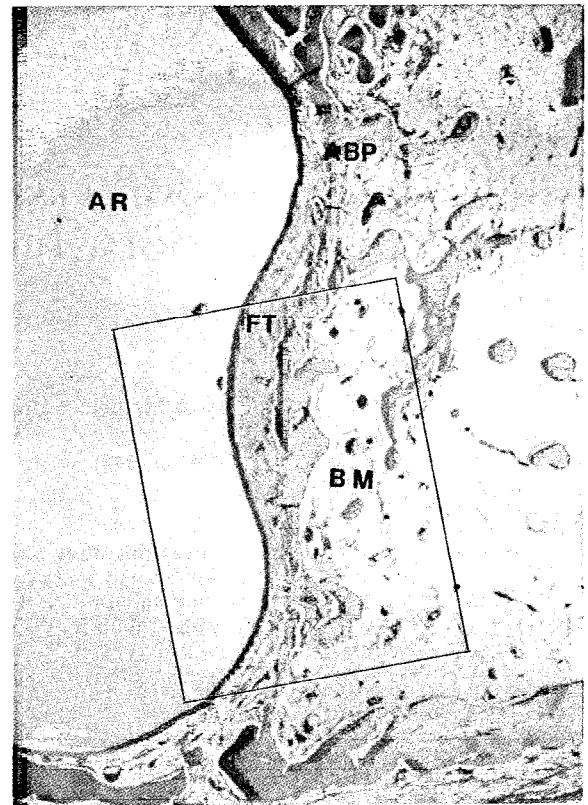


Fig. 2. Area around artificial root 8 weeks after implantation. No inflammatory findings were observed. Good formation of bone resembling alveolar bone proper is observed with fibrous connective tissue of constant width between bone and artificial root (decalcified specimens, HE staining, original magnification $\times 20$). BM — bone marrow; ABP — alveolar bone proper; FT — fibrous tissue. The inset area is shown magnified in Fig. 5.

formation, the original root-supporting tissue, including the periodontal ligament and alveolar bone proper, was removed completely by enlarging the fossa to the size of the artificial root. These procedures were carried out in a way similar to corresponding human clinical application procedures. Therefore, in a case of adapting an artificial root to larger socket formation, apatite granules (Asahi Optical Co.), 100 μm in size, were applied to the area around the artificial root in order to obtain fixation after operation. Artificial roots were implanted with primary stability in the mandible of dogs. The animals were placed on a soft diet for 2 weeks following implantation for post-operative rest and thereafter were maintained on a solid diet for masticatory function of the artificial root.

For preliminary studies, light microscopic observation of undecalcified specimens 6 weeks after implantation and SEM observation on artificial root surface tissue 24 weeks after implantation were carried out. Light microscopy revealed



Fig. 3. Peri-artificial root tissue 8 weeks after implantation (decalcified specimens, Masson trichrome staining, original magnification $\times 40$). The inset is shown magnified in Fig. 4. FT — fibrous tissue; BM — bone marrow; BV — blood vessel.

formation of fibrous tissue and bone formation around the root, while SEM revealed calcified tissue attaching to the artificial root surface. To ascertain these findings, more precise experimental studies on peri-root tissue formation were carried out. To observe tissue formation, artificial roots with surrounding tissue were extirpated, and decalcified specimens were made after fixed periods (8, 12, 16, and 32 weeks).

To observe calcified tissue formation, the author carried out a long-term experiment. The artificial roots with surrounding tissues were recovered after 31 weeks and 72 weeks of implantation. Undecalcified specimens with polished surfaces for microanalysis by Kevex 8000 and decalcified specimens for light microscopic observation were prepared.

The samples were fixed in 20% formalin and were embedded for undecalcified sections in unsaturated polyester resin (Showa Kobunshi Kaisha, Tokyo, Japan) after dehydration. The embedded specimens were thinly sliced with a crystal cutter (BS-3000, Maruto Co., Tokyo, Japan). For decalcified

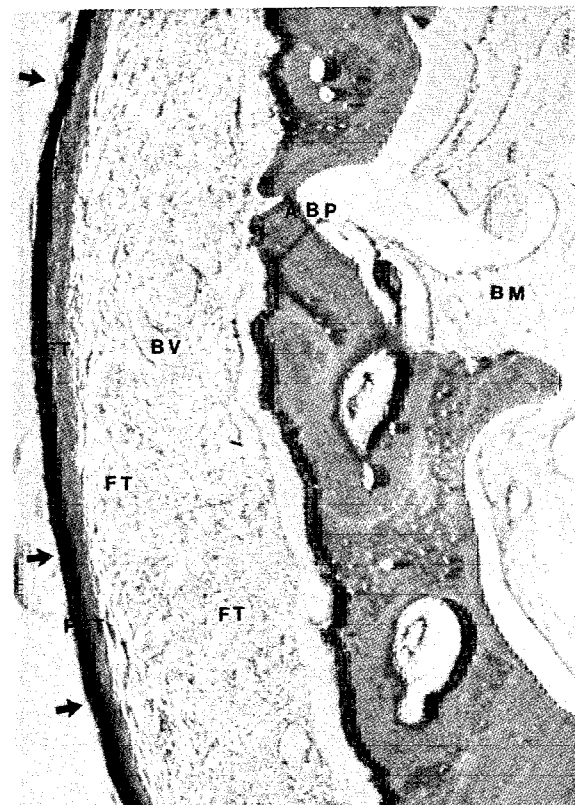


Fig. 4. Peri-artificial root tissue 8 weeks after implantation (decalcified specimens, Masson trichrome staining, original magnification $\times 100$). Fibrous tissue is present between the bone and artificial root via a thin fibrous layer (arrow) running parallel to the artificial root. PFT — parallel fibrous tissue; FT — fibrous tissue; BV — blood vessel; ABP — alveolar bone proper; BM — bone marrow.

specimens, the sections were fixed in 20% formalin, decalcified with diluted hydrochloric acid and formic acid, and embedded in paraffin. Tissue sections $7\ \mu\text{m}$ in thickness were prepared and stained with hematoxylin and eosin, toluidine blue, and Masson trichrome stain, and then observed histopathologically.

The specimens for microanalysis with polished surfaces of undecalcified sections were vaporised with carbon after fixation and dehydration. Then they were analysed by Kevex 8000.

RESULTS

From the preliminary experiment, a peri-implant space of constant width and alveolar bone proper with fibrous tissue, rich in blood vessels, were observed in an undecalcified specimen 6 weeks after implantation (Fig. 1). By SEM of a 24-week-post-operative specimen, the tissue attaching to

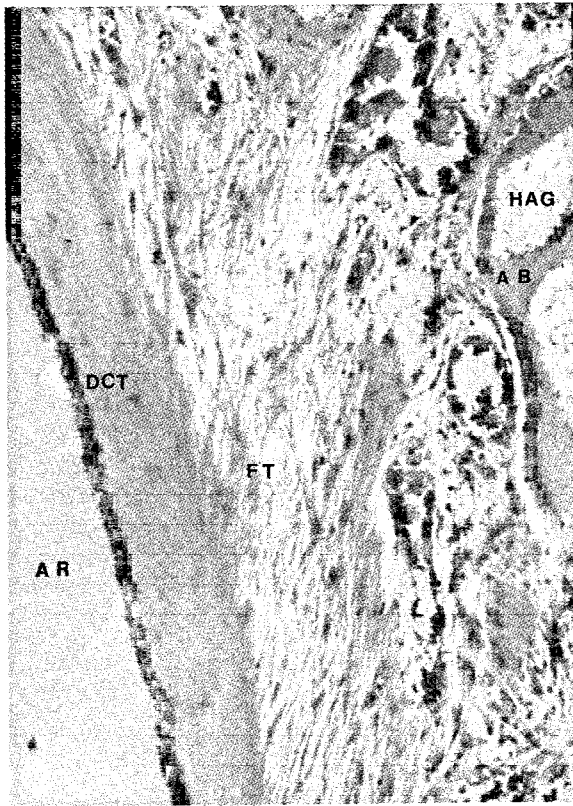


Fig. 5. Peri-artificial root tissue 12 weeks after implantation (decalcified specimens, Masson trichrome staining, original magnification $\times 200$). The thin fibrous layer parallel to the artificial root became more compact with time. HAG — sintered hydroxyapatite granules used in implantation; AB — alveolar bone; DCT — dense compact tissue; FT — fibrous tissue.

the artificial root surface was observed, which was detected as a calcified substance by Fourier-transmitted IR (FTIR) analysis.

From the short-term experiments, the following results were obtained: from 6-week-post-operative specimens, clear epithelial attachment (EA) with functionally orientated fibrous tissue (FT-arrow) was observed without any evidence of inflammation. From 8-week-post-operative specimens, the peri-implant space was filled with thin, parallel, fibrous layers and the perpendicular fibres attaching to both artificial root and alveolar bone proper were observed (Figs 2–4). From 12-week-post-operative specimens, it was observed that parallel fibrous tissue had turned into dense, compact tissue with angled functional fibrous tissue (Fig. 5). The compact tissue observed at the surface of the artificial root had become denser with functional orientation in 16-week-post-operative specimens (Fig. 6). From 32-week-post-operative specimens, it was observed that the dense compact layer attaching to the root surface had turned into dense laminated

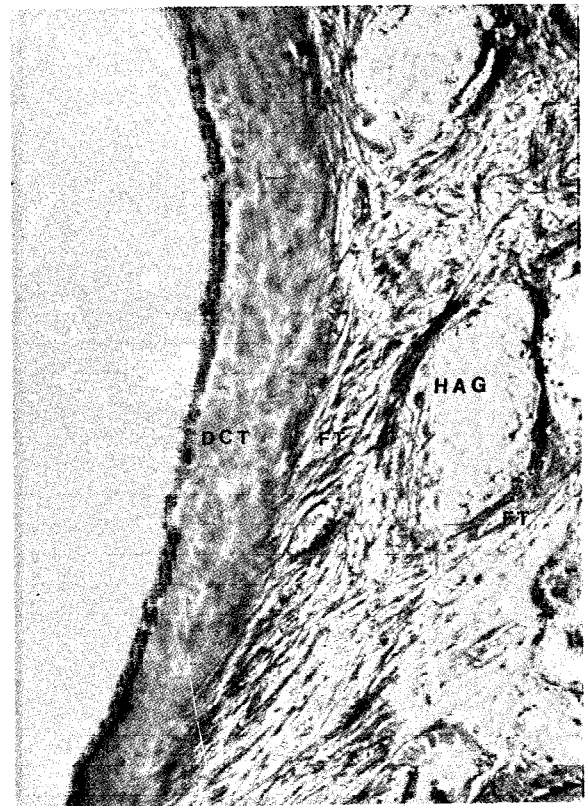


Fig. 6. Peri-artificial root tissue 16 weeks after implantation (decalcified specimens, HE staining, original magnification $\times 200$). DCT — dense compact tissue; HAG — hydroxyapatite granules; FT — fibrous tissue.

tissue with embedded functional fibrous tissue (Fig. 7).

From the long-term experiments (72 weeks after implantation), the following results were obtained: in an undecalcified specimen, calcified substance (CS) with cellular components was observed attaching to the artificial root surface with functionally orientated fibrous tissue (FT) (Fig. 8). At an earlier stage (31 weeks after implantation), the surface of the artificial root was found to have become porous (seen by SEM observation of an undecalcified polished specimen with a microanalyser Kevex 8000 (Fig. 9)). At a later stage (72 weeks after implantation), observation of the undecalcified polished surface by SEM with a microanalyser Kevex 8000 also revealed a calcified substance with cellular components attaching to the hydroxyapatite artificial root surface (Fig. 10). The interface between the artificial root and calcified tissue was found to be porous (Figs 9–10). Energy-dispersive-X-ray maps also revealed a substance rich in calcium and phosphate at the interface between the artificial root and surrounding fibrous or oss-

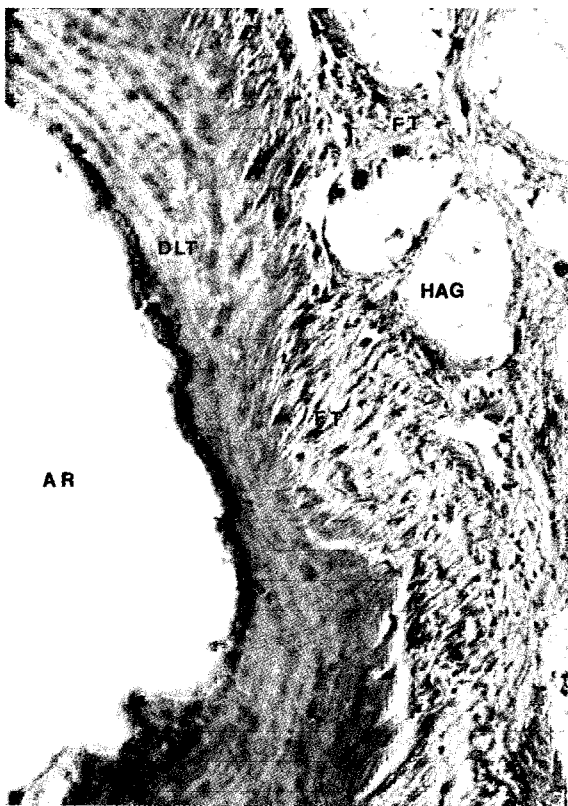


Fig. 7. Peri-artificial root tissue 32 weeks after implantation (decalcified specimens, Masson trichrome staining, original magnification $\times 200$). Dense tissue attached to artificial root surface is laminated. DLT — dense laminated tissue; FT — fibrous tissue; HAG — hydroxyapatite granules.

eous tissues. The interface substance was analysed as calcified tissue denser than bone but less dense than the hydroxyapatite artificial root (Fig. 11).

From these experiments, the following results were obtained: around the new type hydroxyapa-

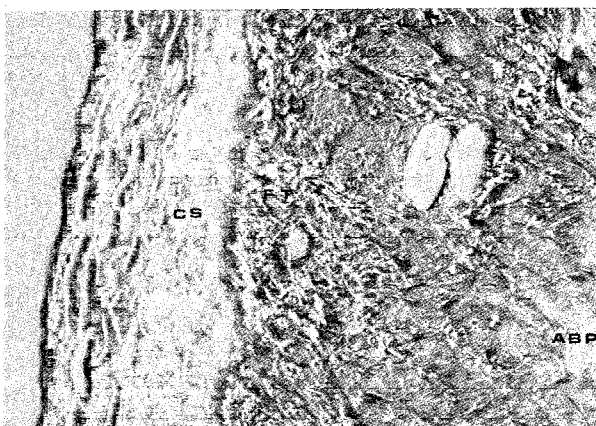


Fig. 8. Peri-artificial root tissue 72 weeks after implantation (decalcified specimen, MT staining, original magnification $\times 200$). Dense laminated tissue assumed to become calcified with angled fibers. CA — calcified substance; FT — fibrous tissue.

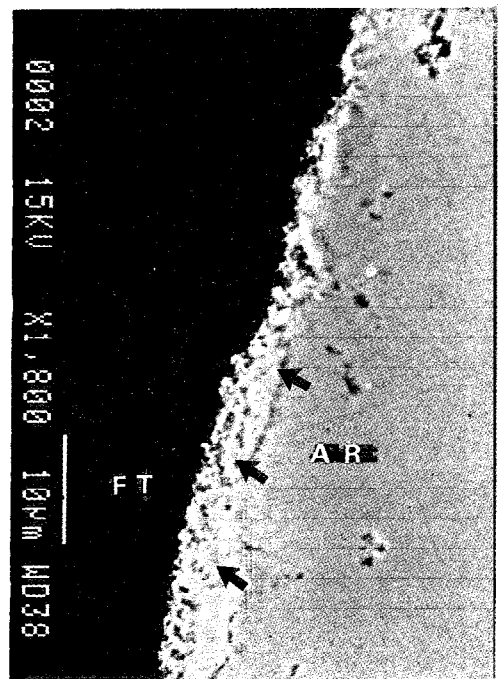


Fig. 9. The surface of artificial root was found to have become porous (arrows) 31 weeks after implantation, as observed by SEM in undecalcified polished specimen. FT — fibrous tissue.

tite artificial root a peri-implant space with fibrous tissue resembling periodontal space, calcified substance resembling the cementum, and bone formation resembling the alveolar bone proper were observed. The orientation of fibrous tissue attaching to the artificial root surface was different at the site of the root configuration. Figure 12 is a scheme of the orientation of fibrous tissue around the artificial root observed in this experiment. The thin fibrous layer attaching parallel to the root surface was found by FTIR and microanalyser to be calcified after long-term function.

DISCUSSION

Presently, many fine ceramics with good biocompatibility are increasingly being put to practical use.^{1-6,10-12} Noting their cellular attachment, the author tried to devise an artificial root made of dense hydroxyapatite with a smooth surface which could attach to fibrous connective tissue without producing osseous adhesion. In this experiment, good periodontal space formation and peri-root tissue formation, i.e. alveolar bone proper with functionally orientating fibrous tissue, was observed (Figs 1-5).

From the morphology of the tissue adjacent to a

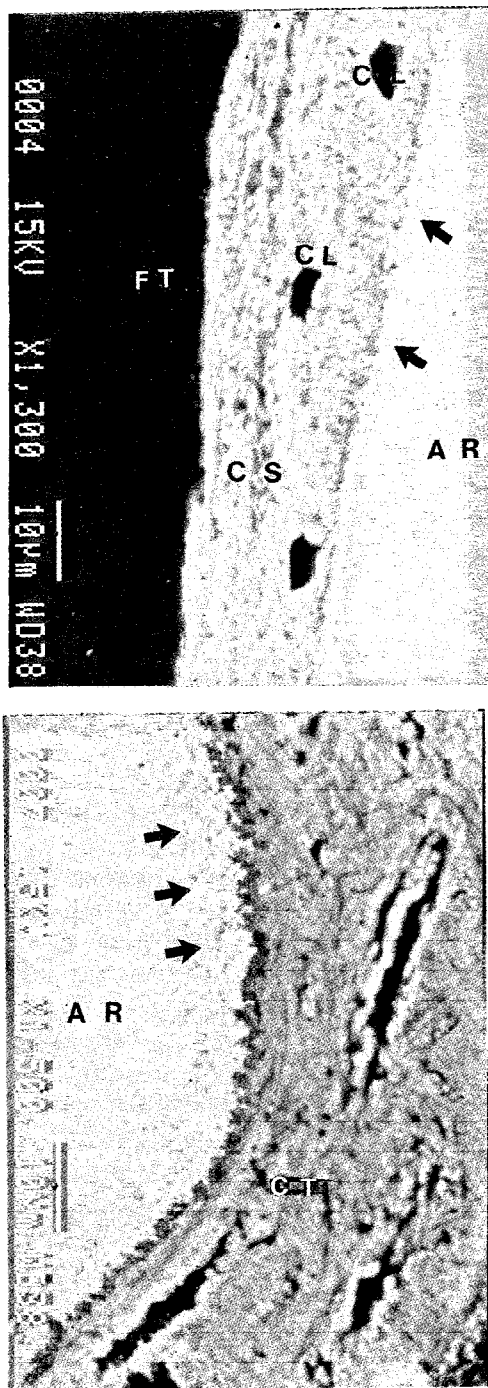


Fig. 10. Cellular calcification is observed by SEM on interface area between artificial root and surrounding tissue of undecalcified polished specimen 72 weeks after implantation. Calcified tissue attaching to root surface with cellular lumens resembles cementum. Surface of artificial root was porous (arrows). CS — calcified substance; FT — fibrous tissue; CL — cellular lumen; AR — artificial root; CT — calcified tissue.

natural tooth or dental implant, the new type of hydroxyapatite artificial root resembles scheme (c) in Fig. 13, the second type of successful condition.¹⁰ Osseous adhesion or osteointegration type

implants are relevant to Fig. 13(e), which is not normal, according to Williams.¹⁰

The author has applied the new type of hydroxyapatite artificial roots clinically with favourable results, and reported on this already at the Third International Congress of Implantology and Biomaterials in Stomatology⁸ (Osaka, 1988), the Fifth Biennial Congress of the International Association of Oral Pathologists (Tokyo, 1990), the Third and Fourth International Symposia on Ceramics in Medicine^{9,13} (Terre Haute, 1990, London, 1991), and the First International Symposium on Apatite (Mishima, 1991). In clinical application, the longest follow-up duration was 61 months. The lamina dura formation with functionally orientated trabeculae could be observed by radiography. These radiographic findings indicated favourable bone remodelling around artificial roots under sufficient masticatory function.

The shape of mammalian dental crown and roots varies according to their site in the jaws. It is also known that the shape of the crown and root varies according to the nature of the species' specific natural diet. This fact indicates that teeth have anatomical configurations related to their function. It also suggests that teeth possess some mechanism which disperses the multidirectional forces evoked by mastication. Considering these points, researchers have to investigate such a mechanical organ as the dental root from combined aspects of morphology (shape effect), material component (material effect), and functional force applied (functional effect).¹⁴ From this point of view, the author together with a co-researcher analysed numerically the shape effect of the new type artificial root with the aid of the finite element method on the functioning jawbone, comparing the results of analyses with conic, cylindrical, and undurated conic shape roots. The results were reported at the First World Congress of Biomechanics¹⁵ (San Diego, 1990). The author compared the findings of specimens made from animal experiments with the results of finite element analyses (FEA), and the following results were obtained: the pattern of osteogenesis in the specimen was thought to have a close correlation to the moderate stress distribution pattern and to coincide with the principal stress trajectory in the FEA analyses; bone formation according to the principal stress trajectory of functioning bone is relevant to Wolff's Law,¹⁶⁻²¹ lamina dura formation with functionally orientated trabeculae was also observed by X-ray tomograph in clinically applied cases. This orientation of the trabeculae

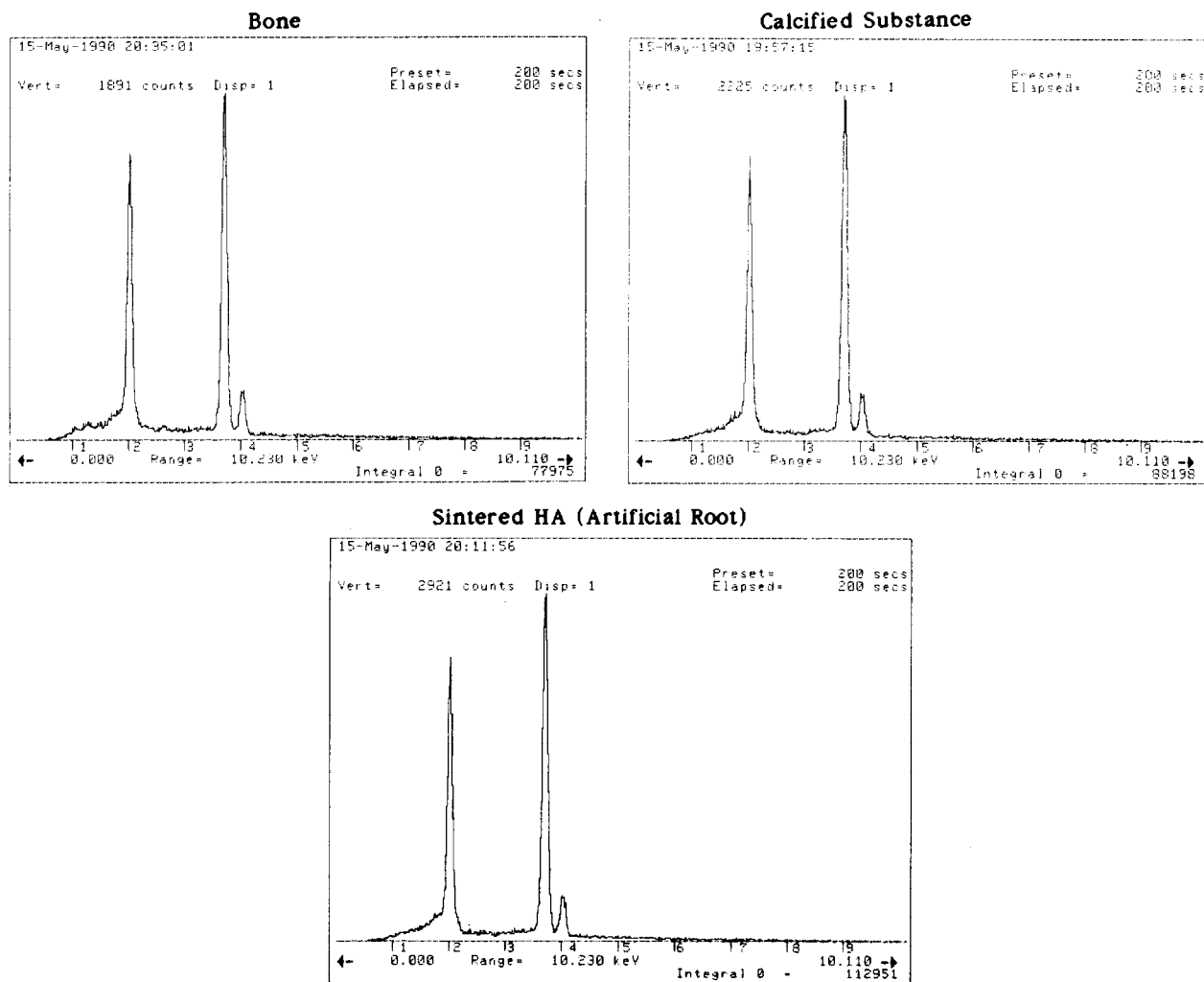


Fig. 11. Analysis patterns by microanalyser showing bone, attaching calcified substance, and sintered dense hydroxyapatite of artificial root. Attaching substance rich in calcium and phosphate, resembling cementum, was analysed as calcified tissue denser than bone but less dense than sintered hydroxyapatite artificial root.

was thought to coincide with the results of FEA. From this FEA study, it is suggested that the shape of the new type artificial root is very suitable biomechanically to form bone tissue resembling alveolar bone proper with the aid of attached fibrous connective tissue around it. The fibrous connective tissue is assumed to play an essential role in forming alveolar bone proper with functionally orientated trabeculae.

In the current experiment, thin parallel fibrous tissue was found in all decalcified specimens in an early post-operative stage (Fig. 4). The parallel fibrous tissue turned into laminated dense layers with time (Figs 5–7), then finally turned into cellular calcification resembling cementum (Figs 8 and 10). In an early post-operative stage, faint angled fibres and thin parallel fibres attached to the root surface were observed (Fig. 4). Comparing the

results of FEA and these histological findings on peri-root fibrous tissue, it is considered that the orientation of collagen fibre has a close correlation to principal stress trajectories. A parallel thin fibrous layer is assumed to form by parallel principal stress trajectories evoked by the functional occlusal force, which is then calcified after long-term function (Figs 8 and 10).

There are essential differences in function between ankylosis and gomphosis in the tooth joint system. Mastication evokes multiple stresses to the tooth. Teeth with mastication function in higher animals require ligamentous joint to the jawbone. On the contrary, the prehensile tooth of reptiles, which has no mastication, is fixed to the jawbone by ankylosis. In this experiment, dogs with artificial roots were placed on a solid diet to give multiple stress against the roots, after 2 weeks rest with

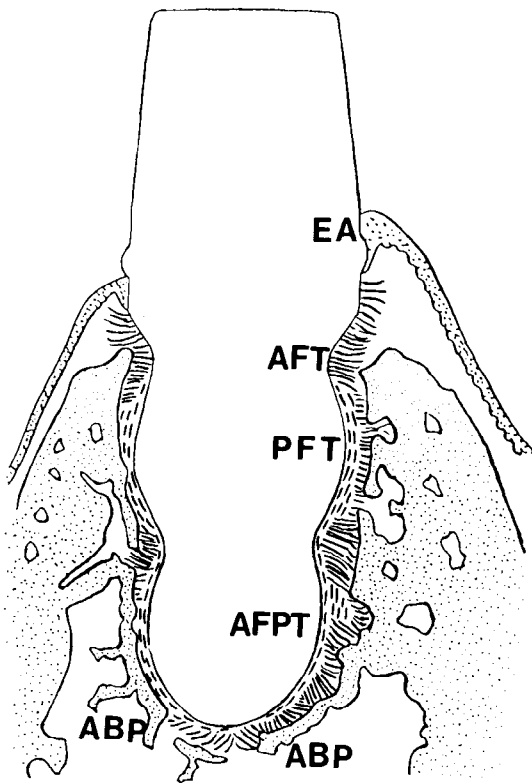


Fig. 12. Scheme of observed specimen, indicating epithelial attachment, formation of alveolar bone proper, and orientation of fibrous tissue attached to artificial root. EA — epithelial attachment; AFT — angled fibrous tissue; PFT — parallel fibrous tissue; AFPT — angled fibers with parallel tissue; ABP — alveolar bone proper.

a soft diet. If the dogs were placed on a soft diet long-term, the implanted artificial root would develop an ankylotic healing.

The author also studied the material effect with the same shape artificial roots made of sintered hydroxyapatite, yttrium-stabilised zirconium oxide, and pure titanium using adult dogs.^{14,22} From these experiments, fibrous tissue attachment and osteogenesis similar to the alveolar bone proper (lamina dura) were observed in all artificial roots regardless of the materials used. However, among the materials observed, hydroxyapatite was unique in that calcified materials resembling cementum were observed by microanalyser and FTIR analyses.¹⁴ From these investigations, the morphology is thought to be the most important factor for artificial roots to have surrounding root supportive bone and fibrous tissue. However, the composition is also important to induce calcified substance resembling cementum.¹⁴

It is reported that periodontal ligament and cementum can only be derived from natural tooth-supporting tissues.⁷ However, it is also known that mesenchymal cells can differentiate to osteoblasts, fibroblasts, periosteum, etc.

Through the experiments described in this paper, there are the following conclusions: (i) By the combined application of three factors to the artificial root, i.e. bioactive materials, proper morphology,

Implantable prostheses

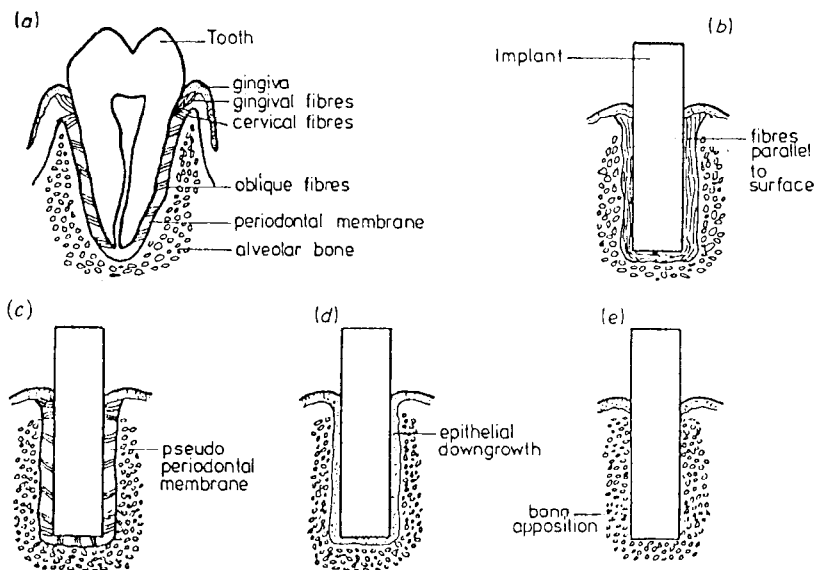


Fig. 13. Scheme of tissue adjacent to natural and dental implants;¹⁰ (a) natural tooth, (b) endosseous implants, with fibrous capsule with fibres parallel to implant, (c) fibres of peri-implant capsule orientated as in periodontal membrane, (d) epithelialisation of endosseous dental implant, and (e) adaptation of bone to dental implant.

and a physiological functioning movement by solid diet mastication, a structure resembling periodontal membrane with cementum-like calcified substance and alveolar bone proper can be formed around the artificial root; (ii) Newly tailored artificial roots can function properly; the cortical bone of the jaw and alveolar bone around the artificial roots are assumed to have been sufficiently remodelled with physiological turn-over in long-term function by the root-supporting structures observed in this study.

ACKNOWLEDGEMENT

The author thanks Mrs Lucille Sakuma for her help.

REFERENCES

1. Kawahara, H., Future vision of implantology. In *Proceedings of International Congress of Implantology and Biomaterial in Stomatology and Japan Society of Implant Dentistry*, Ishiyaku Publishers, Tokyo, 1980, pp. 1–17.
2. Stanley, H.R., Hench, L., Goings, R., Bennett, C., Chellemi, S.J., King, C., Ingersoll, N., Ethridge, E. & Kreutziger, K. The implantation of natural form bioglass in baboons. *Oral Surg. Oral Med. Oral Path.*, **42** (1976) 339–56.
3. Brånemark, P.-I., Osseointegration and 1st experimental background. *J. Prosthet. Dent.*, **50** (1983) 399–410.
4. Aoki, H., Kato, K. & Shiba, M. Synthesis of OH apatite by hydrothermal method, first report. *J. Dent. Appar. Mater.*, **13** (1972) 170–6.
5. Aoki, H. & Kato, K. Synthesis of OH apatite by hydrothermal method, second report. *J. Dent. Appar. Mater.*, **14** (1973) 36–9.
6. Aoki, H. & Kato, K. Application of apatite to dental materials, first report. *J. Dent. Appar. Mater.*, **17** (1976) 200–5.
7. Buster, D., Warrer, K. & Karring, T., Formation of a periodontal ligament around titanium implants. *J. Periodontol.* **61**(9) (1990) 597–601.
8. Nishihara, K. Development and clinical application of natural-type hydroxyapatite artificial roots. *Oral Implantol. Biomater.*, ed. H. Kawahara. Elsevier Science Publishers B.V., Amsterdam, The Netherlands, 1988, pp. 41–6.
9. Nishihara, K. & Akagawa, T., Clinical applications of hydroxyapatite artificial root of fibrous tissue attachment type. In *Bioceramics* (vol. 4). Butterworth-Heinemann Ltd, London, UK, 1991, pp. 223–30.
10. Williams, D.F. Implantable prostheses. *Phys. Med. Biol.*, **25** (1980) 611–36.
11. D'hoedt, B., Heimke, G. & Schulte, W., Bioinert ceramics in dental implantology. In *High Tech Ceramics*, ed. P. Vincenzini. Elsevier Science Publishers B.V., Amsterdam, The Netherlands, 1987, pp. 219–33.
12. Ducheyne, P., Bioceramics: material characteristics versus in vivo behavior. *J. Biomed. Mater. Res.*, **21** (1987) 219–36.
13. Nishihara, K. & Akagawa, T. Case report on artificial root therapeutics. In *Bioceramics* (vol. 3). Phillips Brothers Printers, USA, 1991, pp. 183–92.
14. Nishihara, K. & Akagawa, T. Comparative studies on periodontal tissue around new type artificial roots made of zirconium oxide, titanium and hydroxyapatite. *Phosphorous Res. Bull.*, **1** (1991) 179–84.
15. Nishihara, K., Akagawa, T., Hara, H. & Nakagiri, S., Stress Analysis Related to Artificial Roots of Connective Tissue-Adhesive Type. Abstract of the First Congress of Biomechanics, AMES-Bioengineering, University of California, San Diego, CA, USA, 1990, p. 114.
16. Wolff, J., Über die innere Architektur der Knochen und ihre Bedeutung für die Frage vom Knochenwachstum. *Archiv für pathologische Anatomie und Physiologie und für klinische Medizin. Virchows Archiv.*, **50** (1987) 389–453.
17. Wolff, J., Die Lehre von funktionellen Pathogenese der Deformitäten. *Archiv für Klinische*, **53** 4 (1884) 831–905.
18. Wolff, J., Ueber die Theorie des Knochenwundes durch vermehrten Druck und der Knochenabbildung durch Druckentlastung. *Archiv. für Klin. Chirurgie*, **42** (1891) 302–24.
19. Huiskes, R., Weinans, H., Grootenboer, H.J., Dalstra, M., Fudala, B. & Slooff, T.J. Adaptive bone remodeling theory applied to prosthetic design analysis. *J. Biomechanics* **20**(11, 12) (1987) 1135–50.
20. Fyhrie, D.P. & Cater, D.R., A unifying principle relating stress to trabecular bone morphology. *J. Orthopaedic Res.*, **4** (1986) 304–17.
21. Cowin, S.C., Wolff's law of trabecular architecture at remodeling equilibrium. *J. Biomech. Engng*, **108** (1986) 83–8.
22. Nishihara, K., Kobayashi, T. & Akagawa, T., Studies on periodontal tissue around a new type hydroxyapatite artificial root. In *Bioceramics* (vol. 3). Phillips Brothers Printers, USA, 1992, pp. 171–81.